JOURNAL OF GEOPHYSICAL RESEARCH, VOL. 106, NO. D24, PAGES 33,853–33,866, DECEMBER 27, 2001

Multiyear accumulation and temperature history near the North Greenland Ice Core Project site, north central Greenland

C. A. Shuman[1]
NASA Goddard Space Flight Center, Oceans and Ice Branch, Greenbelt, Maryland, USA

D. H. Bromwich
Byrd Polar Research Center, Ohio State University, Columbus, Ohio, USA

J. Kipfstuhl and M. Schwager
Alfred-Wegener-Institut-fur-Polar-und Meeresforschung, Bremerhaven, Germany

Abstract. This paper presents a comparison of two independent methods of estimating subseasonal accumulation across the interior of Greenland. These methods, high-resolution snow pit studies and atmospheric modeling, have differing spatial and temporal resolution, but both can estimate net accumulation for subseasonal and shorter periods. The snow pit approach is based on a documented relationship between high-resolution snow pit profiles of oxygen stable isotope ratio ($\delta^{18}O$) and multiyear Special Sensor Microwave/Imager (SSM/I) 37-GHz brightness temperature records. Comparison of SSM/I data to profiles obtained during the 1995 Alfred Wegener Institut North Greenland Traverse field season shows that $\delta^{18}O$ data from snow in north central Greenland are a reliable, high-resolution temperature proxy. This enables determination of accumulation amount, rate, and timing from approximately July 1991 through June 1995 across this 220-km-long transect of the ice sheet. Precipitation estimates derived from early modeling based on European Centre for Medium-Range Weather Forecasts data show a similar average seasonal pattern but a diminished magnitude of accumulation (~56%) for these sites. The slope of the multiyear T versus δ correlation was evaluated for each site on the basis of the observed and calculated temperature history from the nearby North Greenland Ice core Project (NGRIP) site automatic weather station. These data should assist interpretation of the paleoclimatic record in the NGRIP deep core.

1. Introduction

Previous research on stable isotope thermometry conducted in Greenland demonstrated the similarity of stable isotope ratio ($\delta^{18}O$ and δD) data from snow pit profiles to multiyear satellite brightness temperatures [*Shuman et al.*, 1995a, 1998]. Those studies found a strong correspondence between stable isotope profiles and multiyear, daily averaged brightness temperature records in central Greenland. A distinctive, multi-peaked temperature cycle observed with the longer-term satellite temperatures, and confirmed with automatic weather station (AWS) data, was substantially preserved in the $\delta^{18}O$ and δD records. The similarity between these two types of temperature data, despite anomalous events and isotopic diffusion, supported the assertion that accumulation occurs at many times throughout the year and that isotopic profiles contain a temperature history with subseasonal resolution. Because of the value of accumulation timing information derived from this technique, we concluded that additional comparisons using this technique should be made. As a further test, this paper will compare accumulation histories from the snow pits to results from high-resolution atmospheric modeling. This paper provides additional analyses and support for the match point technique.

2. Background

Since the time of the first scientific studies in Greenland during the early twentieth century, scientists have struggled to understand climatic conditions on the ice sheet and the factors controlling them [see, e.g., *Loewe*, 1936]. In the latter half of the twentieth century, stable oxygen and hydrogen isotope ratio data from polar ice sheet sites were utilized as a temperature proxy in support of climate interpretation and reconstruction [*Benson*, 1962; *Dansgaard*, 1964; *Dansgaard et al.*, 1973; *Hammer et al.*, 1978]. Early successes have led to the pursuit of more difficult questions as the details on isotopic sources, transport, delivery, and preservation are now known to be complex [*Epstein and Sharp*, 1965; *Johnsen*, 1977; *Kato*, 1978; *Fisher et al.*, 1983; *Johnsen et al.*, 1989; *Petit et al.*, 1991; *Charles et al.*, 1994; *Jouzel et al.*, 1997; *Grootes and Stuiver*, 1997; *White et al.*, 1997]. However, it is clear that records of $\delta^{18}O$ and δD from ice sheet locations provide critical evidence of climate variations [*Johnsen*, 1977; *Hammer et al.*, 1978; *Dansgaard et al.*, 1985; *Johnsen et al.*, 1989; *Cuffey et al.*, 1994;

[1]Also at Earth System Science Interdisciplinary Center, University of Maryland, College Park, Maryland, USA.

Paper number 2001JD900197.
0148-0227/01/2001JD900197$09.00

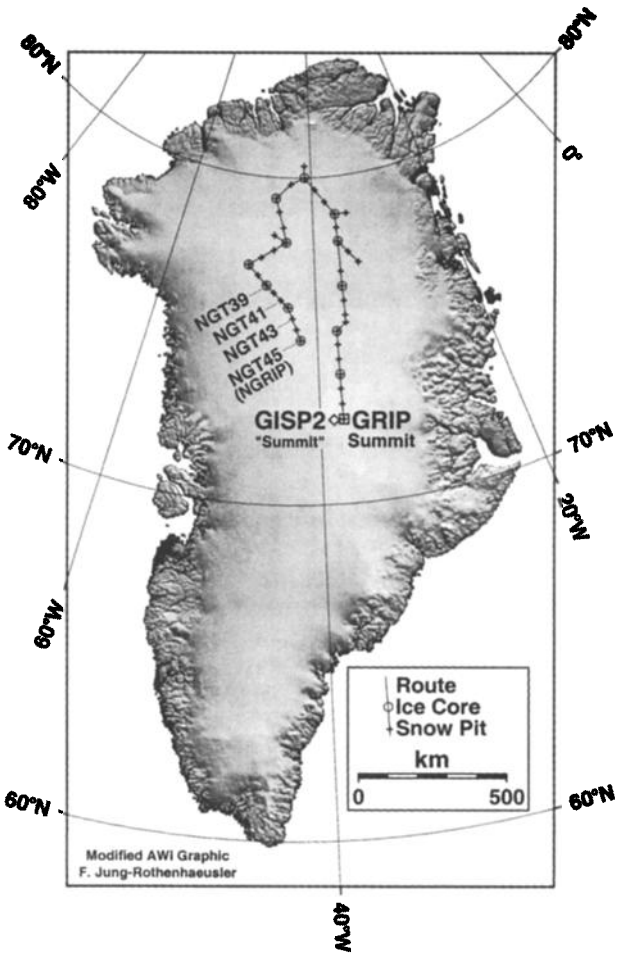

Figure 1. Illustration of the Alfred Wegener Institut (AWI) North Greenland Traverse (NGT) route (1993–1995) as well as the location of the four snow pits (NGT39, NGT41, NGT43, and NGT45) studied here. The locations of the three Greenland deep ice core projects referred to in the text are also identified.

Jouzel et al., 1997]. Recently, diverse investigations into the mass balance and climatic history of the Greenland ice sheet (NASA Program for Arctic Regional Climate Assessment (PARCA) and Alfred Wegener Institut North Greenland Traverse (AWI NGT)) over timescales ranging from years to centuries have utilized $\delta^{18}O$ and δD data [*Abdalati et al.*, 1998; *Fischer et al.*, 1998a, 1998b, 1998c]. Despite uncertain knowledge of factors influencing the stable isotope content of snow and ice [*Jouzel et al.*, 1997; *Grootes and Stuiver*, 1997] these records are crucial to understanding this part of the global climate system.

3. Methodology

This study utilizes high-resolution stable isotope profiles (3-cm incremental samples or ~15–20 samples per year [*Schwager*, 1999]) taken at four sites along the 1995 AWI NGT route (see Figure 1). These profiles are "matched" to multiyear, passive microwave brightness temperature (T_B) records from the pixels covering each site. These T_B data are obtained from one of several passive microwave sensors that have been gathering data over the polar regions more or less continuously since 1978. The T_B data are converted to an estimate of absolute temperature by short-term AWS data from the North Greenland Ice Core Project site (NGRIP, ~15 km from NGT45). The use of the match point technique allows (1) the subseasonal variation of the isotope record in the near-surface snow to be temporally constrained, (2) the slope of the T versus δ correlation to be evaluated, (3) in situ measurement of the amount and timing of accumulation for subseasonal to annual periods, and (4) independent validation of accumulation estimates derived from atmospheric models (mass input P from *Chen et al.* [1997]). A specific goal of this project was a month-by-month assessment of the precipitation amounts estimated by the model for interior ice sheet locations in order to assess the tremendous potential of this type of accumulation data. An additional goal was to derive information regarding the T versus δ relationship. These combined results should encourage application of this approach at other ice sheet locations where satellite passive microwave observations can provide a record for detailed comparison to stable isotope profiles.

Table 1. AWI NGT Snow Pit Data[a]

Pit Name	Depth, m	Latitude, °N	Longitude, °W	Elevation, m	Date
NGT39	2	76.66	46.48	2733	June 20, 1995
NGT41	2	76.24	44.49	2858	June 26, 1995
NGT43	2	75.66	42.98	2921	June 29, 1995
NGT45	2	75.00	42.00	2947	July 6, 1995

[a]The 1995 summer season pit profiles are courtesy of researchers on the North Greenland Traverse of the Alfred Wegener Institut (AWI NGT), Bremerhaven, Germany. GPS instruments determined pit locations and elevations.

3.1. Stable Isotope Data

The in situ basis of this study is a series of high-resolution $\delta^{18}O$ records from snow pits [*Schwager*, 1999]. They were obtained during June and July 1995 along an ~220-km traverse route north-northwest of the current NGRIP deep core site (see Table 1 and Figure 1). The pit data included high-resolution sampling for stable oxygen isotopes and stratigraphic interpretation. The snow pits were dug in "clean" areas to a depth of ~2 m and were sampled at 3-cm resolution using standard field procedures for isotopes. The samples were analyzed at the AWI isotope laboratory with uncertainties of better than ±0.5‰ relative to standard mean ocean water (SMOW).

To aid comparison to the T_B data, the $\delta^{18}O$ profiles are presented as if they represent a time series of δ values even though they actually represent discrete snowfall events that are subject to reworking, diffusion, and diagenesis during and for some time after burial. Although diffusion is known to change isotopic values contained in snow and ice [*Dansgaard et al.*, 1973; *Johnsen*, 1977; *Whillans and Grootes*, 1985; *Sommerfeld et al.*, 1991; *Friedman et al.*, 1991; *Johnsen et al.*, 1999, 2000], in this study, no attempt has been made to adjust these isotope values for diffusion effects. At the moment, there is no precise way to account for diffusion, especially in the absence of detailed physical snowpack data, although efforts are being made [*Shuman et al.*, 1995a].

Figure 2 illustrates the generally consistent relationship between each adjacent pit's isotope stratigraphy during the early 1990s. The temporal correlation between the profiles is indi-

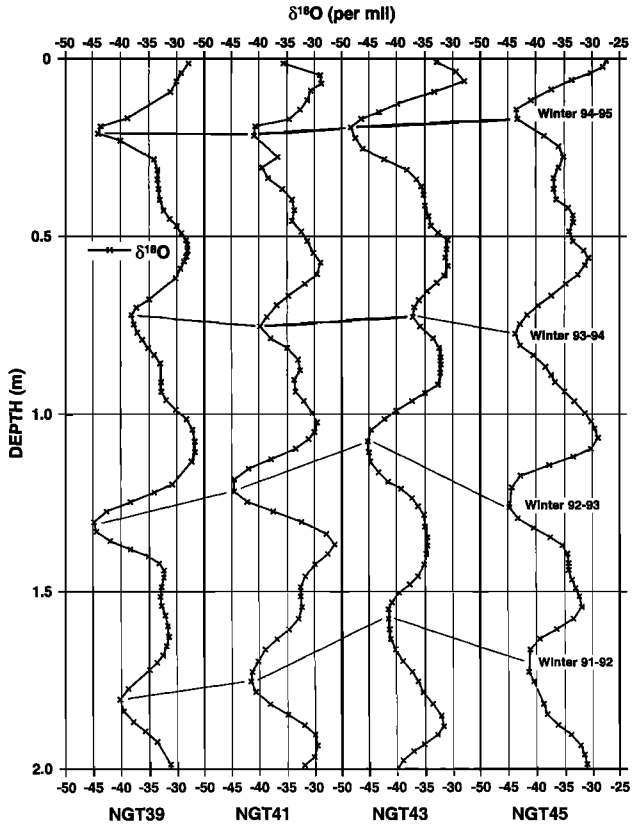

Figure 2. Comparison of four high-resolution NGT $\delta^{18}O$ profiles that form the basis of this paper. The general stratigraphic relationships are indicated by tie lines indicating the approximate times of the more negative isotope winter periods.

cated relatively by the lines between their respective winter periods. The depth of any given temporal horizon roughly indicates the amount of accumulation, with a deeper horizon indicating relatively higher accumulation. In general, the NGT39 pit appears to have the highest accumulation, followed by the nearly equivalent NGT45 and NGT41 sites, with NGT43 having the lowest accumulation overall. Density data were available only from core sites in this area [*Schwager*, 1999], so determination of water-equivalent accumulation values is less precise.

3.2. Passive Microwave Data

The passive microwave data used for comparison to the isotope profiles were extracted from the *National Snow and Ice Data Center* (*NSIDC*), 1992] CD-ROMs. Daily averaged, 37-GHz, vertical polarization (V), brightness temperatures (T_B) from the Special Sensor Microwave/Imager (SSM/I-F11) for the 25 × 25 km grid cell covering each NGT site were compiled to document the multiyear "temperature" trend for the site. Brightness temperature data from the 37-GHz V (0.81 cm wavelength) channel begin in December 1991 and extend to the present day. The measurement accuracy of the SSM/I 37-GHz V channel is ±2 K [*Hollinger et al.*, 1990].

The relationship of T_B to physical temperature is described by the Rayleigh-Jeans approximation [*Hall and Martinec*, 1985]. Satellite T_B is primarily a function of the physical temperature of the near-surface snow (T) multiplied by its emissivity (ε) (or $T_B \sim T \times \varepsilon$). Atmospheric effects on brightness temperature are ignored because of the low temperatures and limited water vapor content found in this area [*Maslanik et al.*, 1989]. For dry snow, emissivity is controlled primarily by radiative scattering from the ice grains over a skin depth of a meter or so for the 37-GHz channels but is dominated by the top 20–30 cm [*Rott et al.*, 1993]. This depth is roughly equivalent to that of the diurnal temperature cycle [*Alley et al.*, 1990]. Overall, the emissivity of the snow and ice is controlled primarily by grain size [*Chang et al.*, 1976; *Armstrong et al.*, 1993], which tends to vary over an annual period [*Benson*, 1962], although layering and other factors also contribute.

The reason for demonstrating the relationship of the $\delta^{18}O$ data to the SSM/I T_B values instead of directly to observed air temperature is simple. The number of AWS temperature sensors on the Greenland and Antarctic ice sheets is quite limited, and their period of record is usually short and/or intermittent [*Shuman et al.*, 2000]. However, T_B data are available more or less continuously since late 1978, and the coverage region of the current SSM/I sensor includes all of Greenland and all but ~3° of latitude at the South Pole [*NSIDC*, 1992; *Hollinger et al.*, 1990]. Therefore snow pit and shallow ice core stable isotope records can be usefully compared to T_B records to determine accumulation timing even if they lack short-term AWS temperature (T_A) records for calibration. As demonstrated in section 3.3, AWS T_A data can be used to calibrate, with some limitations, a much longer passive microwave record for a site, using emissivity modeling. It must be mentioned that T_B records are strongly influenced by the presence of liquid water in the near-surface snow [*Abdalati and Steffen*, 1997; *Zwally and Fiegles*, 1994]. Consequently, isotope profiles can be best compared to T_B records at sites where melt events are rare or nonexistent.

3.3. Calibrated Brightness Temperatures

As first described by *Shuman et al.* [1995b], 37-GHz V brightness temperature (T_B) data can be related to near-surface AWS air temperatures (see Figure 3). The 37-GHz V data are used for this technique because they provide the best correlation of the available long-term passive microwave channels with the AWS mean daily air temperature data [*Shuman et al.*, 1995b]. Some difficulties in the utilization of this technique were documented by *Shuman et al.* [1998] for central Greenland. Those problems were specifically related to temporal variations in near-surface emissivity due to hoar formation [*Shuman and Alley*, 1993; *Shuman et al.*, 1993; *Abdalati and Steffen*, 1998] and to the extrapolation of an approximate emissivity cycle prior to the period supported by AWS data. Additional difficulties for this effort were presented by the temporal separation of AWS temperature observations from the time period represented by the isotope profiles and the physical separation of the NGRIP AWS from the most distant site (NGT39).

Conversion of the SSM/I T_B data for each NGT site to near-surface air temperature (T_C) values was achieved through the use of an empirically derived emissivity function which is based on the Rayleigh-Jeans approximation (see section 3.2 and *Shuman et al.* [1995b]). Basically, short-term AWS temperatures (T_A) are substituted in place of the near-surface snow temperatures, ratioed with temporally equivalent T_B data, and used to generate an approximate emissivity (ε) time series. A sinusoid is then fitted to the approximate emissivity data (T_A/T_B) using Igor® software to define a modeled emis-

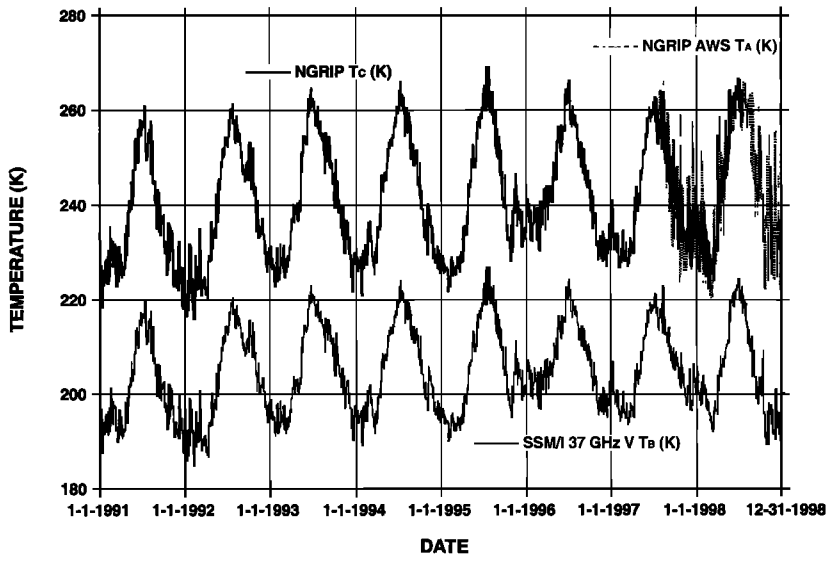

Figure 3. Illustration of the calculated air temperature (T_C) record generated using the observed daily averaged AWS air temperature (T_A) record from the NGRIP AWS and SSM/I 37-GHz V brightness temperature (T_B) data from the NGT45 site. The T_C data are generated using modeled emissivity cycles to calibrate the T_B time series (see technique of *Shuman et al.* [1995b]). There is close association of the T_C data to the overall T_A trend in 1997–1998, despite short-term air temperature variations.

sivity cycle during the period when both T_B and T_A data are available. The emissivity sinusoid is then used to "calibrate" the T_B data into an estimated near-surface air temperature (T_C) record that corresponds closely to the trend in T_A (for further discussion of the technique, including error analyses, see *Shuman et al.* [1995b, 2000]. In this study, it was assumed that the emissivity cycle was temporally stable to allow temperature history development. Figure 3 illustrates how this approach was used to calibrate the SSM/I 37-GHz V T_B data for the NGT45 site using data from the nearby NGRIP AWS (available at http://cires.colorado.edu/steffen/gc-net.html) [*Steffen et al.*, 1996].

As documented by *Shuman et al.* [1998], the modeled emissivity cycle is not always stable. This appears to be the case here as the NGRIP T_C record diverges significantly from a composite temperature record at the Greenland Ice Sheet Project (GISP) 2 or "Summit" site (~300 km away) prior to the summer of 1992 [*Shuman et al.*, 2000]. Following the summer of 1992, the composite T_C record for NGRIP appears generally similar to the Summit record with reduced difference statistics. Examination of the T_C trend (Figure 3) during the AWS overlap period suggests these calibrated data are less sensitive to short-term, high-frequency fluctuations in temperature which is due to the reduced sensitivity of the T_B data [*Shuman et al.*, 1995b]. It is also important to note that the AWS record is temporally separated from the snow pit records by more than 2 years (see Figure 3) and is spatially separated from the farthest NGT site by hundreds of kilometers (see Figure 1). Unfortunately, there is no other way to generate a daily near-surface temperature history for these sites. In any event, it is important to keep in mind that the temperature data have a degree of uncertainty.

3.4. Atmospheric Modeling

Polar accumulation estimates derived from the modeling of climate analysis data have the advantage of a synoptic view and explicit temporal control [*Bromwich et al.*, 1998, 1993]. Another advantage is that the risks of field data acquisition are effectively eliminated. However, model output requires validation by independent means to ensure confidence, and in situ accumulation data are necessary to do this. There are spatial scale issues to consider, as comparing results from a model grid cell, even at the best available resolution, to a snow pit or an ice core record is not an exact match [*McConnell et al.*, 2000]. This problem may be exaggerated by the location of the field site within a grid cell; this problem can also affect calibration of T_B grid data using a single AWS. Temporal differences are also likely, as field data on accumulation cannot be dated as confidently as a model. However, by tailoring the model output interval to the spatial and temporal coverage of a series of snow pits, as is the case here, these types of accumulation data should be closely compatible.

The accumulation output utilized here is derived from an evolving series of modeling efforts that have been extensively intercompared for Greenland [*Bromwich et al.*, 1998]. The data examined in this effort are derived from the Chen-Bromwich model [*Chen et al.*, 1997], which is based on 12-hourly European Centre for Medium-Range Weather Forecasts (ECMWF) operational analyses. The grid pixels are ~50 km on a side, and the data utilized here cover the time period 1991 through 1995. The dynamic precipitation retrieval method used by these models to calculate mass input (P) are discussed thoroughly by *Bromwich et al.* [1998] and *Chen et al.* [1997]. (It is important to note that the ECMWF fields suggest that evaporation/sublimation (E) is small and is consequently assumed to be inconsequential by the modeling approach. As a result, in the model context, precipitation equals accumulation.) Validation efforts presented by *Bromwich et al.* [1998, Table 2] indicate that Chen-Bromwich-modeled interannual accumulation values are ~50% of the observed accumulation in the high interior of Greenland. These results are similar to those of *McConnell et al.* [2000], which show a similar magnitude problem for annual accumulation estimates. Improvements to the

modeling approach are discussed by *Bromwich et al.* [this issue]. This paper will focus on comparisons of intra-annual accumulation from both field and modeling data but will also compare annual values as presented in more typical accumulation maps [*Bales et al.*, 2001].

4. Results

As in the studies near the GISP 2 (now Summit) site (see Figure 1), this paper is based on match points made using a qualitative, point-pairing procedure between the microwave T_B records and the $\delta^{18}O$ profiles. Primarily, similarities in the shapes of the trends guide selection of the match points. Basically, this involves examining temporally equivalent portions of the two records and making the assumption that the major peaks (maxima), valleys (minima), or intermediate inflexions represent equivalent events in both records. It should be noted that rapid isotopic diffusion or extremely low or strongly seasonal accumulation would hinder this approach but that these issues were not observed here.

The temporally equivalent daily average 37-GHz V T_B record was directly compared to the corresponding isotope record from each NGT site (see Figure 4). In Figure 4, note that variability in the accumulation rate prevents a one-to-one correspondence between the time axis of the T_B records and the depth axis of the $\delta^{18}O$ records. This series of plots shows that the multipeaked temperature cycle observed in the passive microwave record is generally preserved in each snow pit's isotope record. The resulting paired data (depth and associated $\delta^{18}O$ value from the isotope profile as well as the date and calibrated brightness temperature (T_C); see Table 2) provide the basis for the following analyses. Identification of the 15 to 18 match points in each comparison was facilitated by previous knowledge of the approximate accumulation rate in this area from *Ohmura and Reeh* [1991].

The trend comparison of T_B and $\delta^{18}O$ values for these pits shows that the top 2 m of snow corresponds to about four annual cycles. Figure 4 also suggests that equivalent primary and secondary maxima and minima can be found in both proxy temperature records. This suggests that the stable isotope records contained in the pits are derived from snow that has been accumulating at many times, and therefore at different temperatures, throughout the year. It should be noted that although the technique determines a specific match point date for a specific depth in the snow pit, there is a degree of temporal uncertainty associated with these correlations that is difficult to quantify. In addition, it becomes increasingly difficult to match subtle features at deeper (and consequently older) depths along the isotope profiles. This reduces temporal resolution of accumulation in the oldest portion of the study period.

The match point comparisons illustrated in Figure 4 reveal a few periods of anomalous isotopic values in the profiles. These can be identified by distinct differences in the brightness temperature and isotope trend patterns. An example exists at match points NGT41-3 and NGT41-4 where the main summer peak appears cooler than a subsequent isotope maximum. In addition, the profile in the vicinity of match point NGT43-10 suggests that very little accumulation occurred at this location during the winter of 1993–1994. Differential snow accumulation patterns over short distances may account for some of these anomalies, and how well any single profile represents an area is a concern (see Figure 2). Despite this, it appears that the T_B and $\delta^{18}O$ records tend to preserve a primary peak and trough as well as a secondary peak in the fall or early winter in most years. More aggressive analysis and mathematical interpolation could produce other match point pairs but may introduce additional noise to the data [see *Shuman et al.*, 1998, Figure 7].

4.1. Isotope Temperature Relationship

The match point data from Table 2 and the resulting T_C versus $\delta^{18}O$ plot (see Figure 5) illustrate how isotope values compare to (calculated) near-surface air temperatures. The T versus δ slopes for the four sites range from 0.31 to 0.26. These values are substantially lower than the modern spatial gradient slope of 0.67 [*Johnsen et al.*, 1989] and are also lower than the value of 0.50 derived from analyses of the GISP 2 $\delta^{18}O$ and borehole temperature records [*Cuffey et al.*, 1992, 1994]. The slope of the regression line through all data points, 0.28 ± 0.094, is lower than the values (0.46 ± 0.075 and 0.39 ± 0.111) reported for the Summit site using the same technique (*Shuman et al.* [1995a] and *Shuman et al.* [1998], respectively). It is not statistically distinguishable from the second value, however. (All the ± values reported here are for the 95% confidence limit.) Some possible reasons for the variability in slope values will be discussed below.

The T_C versus $\delta^{18}O$ trend in the data for all four sites (Figure 5) is fairly consistent, but outliers exist for some match points in several of the pits. These outliers are probably related to snow derived from distant sources of water vapor, complex isotope fractionation that is not simply temperature driven, in situ diffusion during diagenesis, or even drifting of geographically distant accumulation into the area [*Newell and Zhu*, 1994; *Charles et al.*, 1994; *Jouzel et al.*, 1997]. The periods of anomalous accumulation seen in the general trend comparisons may also be related to these points. The use of the T_C record derived from the NGRIP AWS may also be a factor for the more distant pits. Of course, another possibility is the existence of errors in the application of the match point technique.

4.2. Water-Equivalent Isotope Profiles and Accumulation Data

Quantitative information on accumulation amount and timing can be derived using the match point data and density-corrected (water-equivalent) $\delta^{18}O$ profiles. Because density data were not available for each individual snow pit profile, a high-resolution density profile from the top 2 m of the NGT42 core (between NGT41 and NGT43 and not presented here) was used as the best available data for all four sites. This may also introduce some error into the accumulation histories for the four sites. The resulting water-equivalent depth data for the match points from the Figure 4 trend comparisons are listed in Table 2.

The amount of accumulation for each time interval defined by a pair of match point data can be calculated from the water-equivalent depth profile. The match point dates from the T_B record define the number of days over which the corresponding amount of water-equivalent snow has accumulated and monthly averages were then calculated based on these periods. To minimize introducing bias to the averages, all accumulation amounts from match point time intervals <30 days were merged with the preceding interval. These results are presented as a time series of monthly average accumulation rates (see Figure 6a) to aid comparison to the model results

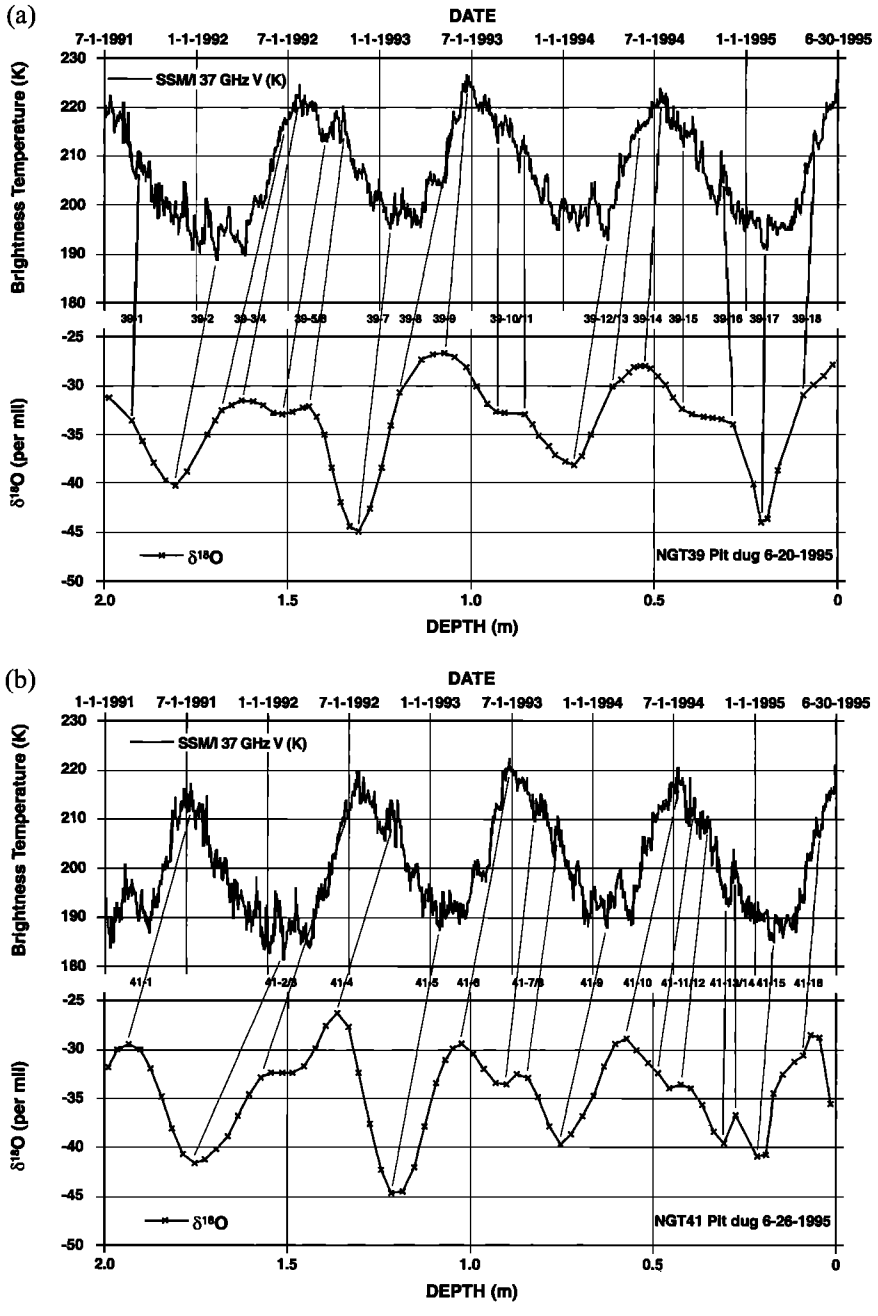

Figure 4. Comparison of SSM/I 37-GHz V brightness temperature data (daily average in kelvins) with the stable isotope record from each of the four 2-m pits (parts per mil in meters). Match points are indicated by tie lines and are numbered sequentially for each snow pit (see Table 2). The comparison of these two proxy temperature records is qualitative and is based on similarities in trend shape. This allows dates to be assigned to specific pit depths and allows accumulation per interval to be determined [see *Shuman et al.*, 1995a, 1998].

that are calculated as month-by-month values (see Figure 6b) from the 12-hourly ECMWF atmospheric data. For consistency, the resulting monthly values from both sources are plotted at the interval midpoint date in Figure 6. (Note that the accumulation data reflect only the net amount over any interval because these time periods must include periods with and without mass input as well as, possibly, periods of mass loss or redistribution. *Gardner et al.* [1987] discuss this process rate problem.)

The rate of accumulation determined by the match point technique clearly varies throughout the year at all four sites (Figure 6a). The range in water-equivalent accumulation rate is from a minimum value of ~6.87 to ~47.37 mm/month with a mean of ~15.85 mm/month. All four sites have generally similar distributions. The lowest monthly accumulation rates (<10 mm/month) tend to occur in the late fall or early winter months. The highest monthly accumulation rates (>20 mm/month) tend to occur in the summer or early fall months. The highest monthly value is derived from a relatively short interval (36 days). The highest accumulation points also occur at the shallowest depths in NGT41, NGT43, and NGT45 and may be due to reduced diffusion and diagenesis as compared to deeper

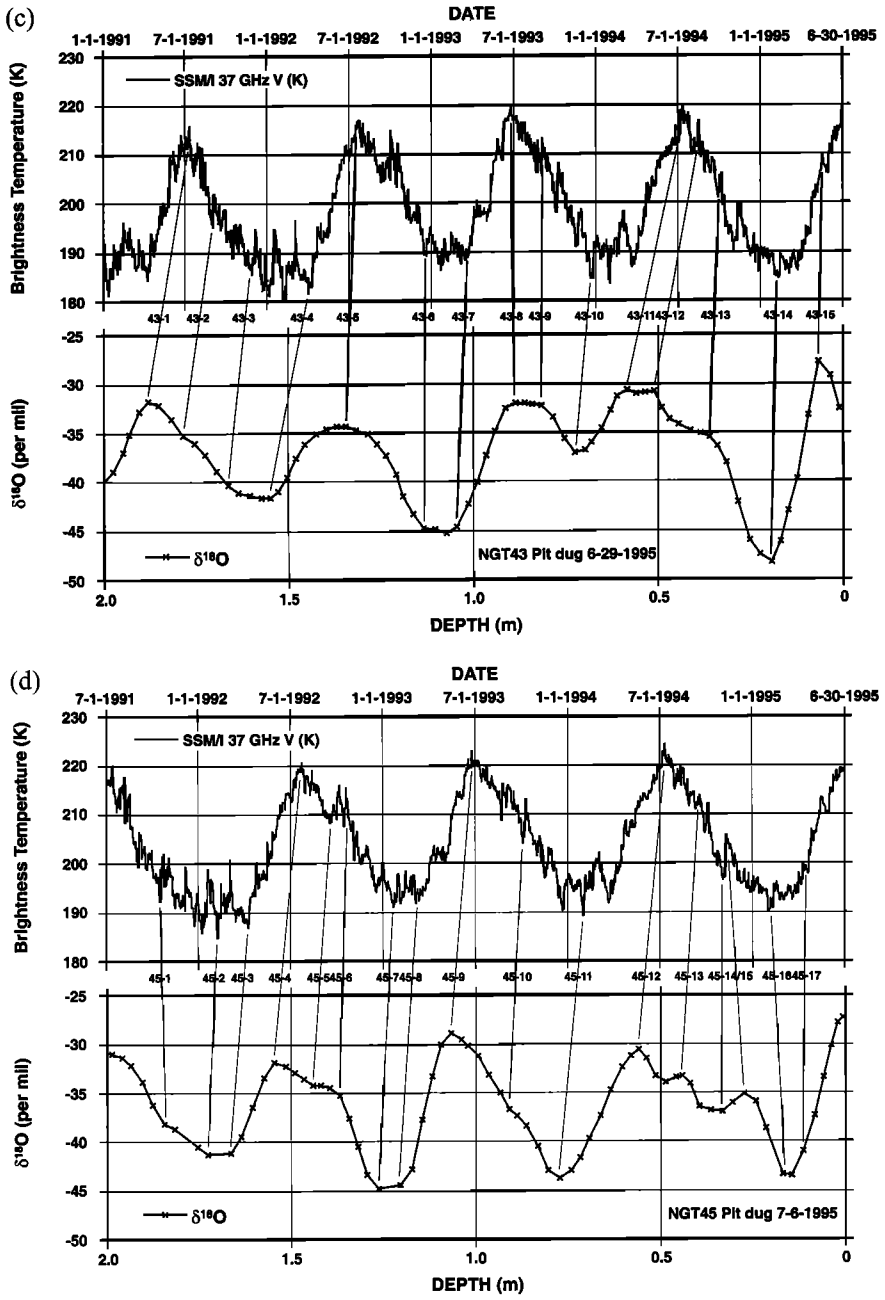

Figure 4. (continued)

parts of the profiles. Longer intervals, more common in the older and deeper portions, tend to have lower monthly accumulation rates for the reasons suggested above. The mean time interval from this application of the match point technique, ~93 days, is slightly longer than in the previous studies.

The rate of accumulation determined by the Chen-Bromwich model also varies throughout the year at all four sites (Figure 6b). These data suggest a strong bimodal distribution to accumulation across the 50-km grid cells in this area. The accumulation rate ranges from a minimum value of ~1.39 to ~32.37 mm/month with a mean of ~8.59 mm/month. The lowest monthly accumulation rates (<10 mm/month) tend to occur in the late fall or early winter months and appear to be more common for the more southerly sites. The highest monthly accumulation rates (>20 mm/month) tend to occur in the summer or early fall months and are more common at the NGT39 site than for sites farther to the south.

Overall, Figure 6 illustrates the relative abilities of the two techniques to resolve subseasonal accumulation. There are clearly differences in magnitude and timing between them. The snow pit approach has lower temporal resolution than the atmospheric modeling approach (~3-month versus 1-month averages). This difference in time resolution is especially apparent in the relatively smoother field results from the older, deeper snow. In addition, temporal control on the match points is less precise deeper in the snowpack. The atmospheric modeling results are relatively more consistent in magnitude at each site but are substantially lower overall than the field data (see Figure 6). Resolving these differences would be beneficial; however, at the moment these two techniques represent the

Table 2. Data on Profile Match Points From Four AWI NGT Snow Pits[a]

Match Point ID	Match Point Date	SSM/I Calculated Temperature, K	$\delta^{18}O$, ‰	Water Equivalent Depth, cm
		Pit NGT39		
Surface	June 20, 1995	262.56	−27.9	0
39-18	May 15, 1995	254.82	−31.0	3.88
39-17	Feb. 8, 1995	222.74	−44.0	8.49
39-16	Nov. 11, 1994	246.20	−33.9	11.75
39-15	Aug. 28, 1994	249.82	−32.4	16.63
39-14	July 12, 1994	265.61	−28.0	19.66
39-13	May 29, 1994	257.73	−30.1	22.78
39-12	March 29, 1994	226.90	−38.1	26.32
39-11	Oct. 12, 1993	250.92	−32.9	30.88
39-10	Aug. 21, 1993	251.25	−32.7	33.48
39-9	June 20, 1993	268.97	−26.7	38.12
39-8	May 25, 1993	259.68	−30.7	42.33
39-7	Jan. 20, 1993	227.56	−44.9	45.80
39-6	Oct. 17, 1992	257.75	−32.2	50.24
39-5	Sept. 6, 1992	250.86	−33.0	52.59
39-4	July 18, 1992	263.59	−31.5	56.24
39-3	June 23, 1992	258.64	−32.6	57.87
39-2	Feb. 8, 1992	220.40	−40.2	62.00
39-1	July 31, 1991	259.63	−33.5	66.33
		Pit NGT41		
Surface	June 26, 1995	257.09	−35.5	0
41-16	May 16, 1995	249.28	−30.5	3.42
41-15	Feb. 9, 1995	216.23	−40.9	8.7
41-14	Nov. 11, 1994	237.92	−36.7	11.21
41-13	Nov. 1, 1994	224.64	−39.5	12.40
41-12	Sept. 14, 1994	247.96	−33.6	16.51
41-11	Aug. 3, 1994	247.11	−32.3	18.51
41-10	July 11, 1994	261.71	−28.9	21.43
41-9	Jan. 30, 1994	219.25	−39.7	27.53
41-8	Oct. 12, 1993	246.82	−32.9	30.42
41-7	Aug. 20, 1993	247.50	−33.6	32.29
41-6	June 24, 1993	264.10	−29.4	36.37
41-5	Jan. 20, 1993	218.47	−44.6	42.82
41-4	Oct. 2, 1992	250.49	−26.3	47.67
41-3	June 24, 1992	253.77	−32.9	54.44
41-2	Feb. 6, 1992	211.82	−41.6	60.24
41-1	July 11, 1991	257.79	−29.5	66.51
		Pit NGT43		
Surface	June 29, 1995	257.79	−32.7	0
43-15	May 16, 1995	248.68	−27.8	2.69
43-14	Feb. 7, 1995	215.59	−48.3	8.13
43-13	Sept. 26, 1994	235.84	−35.5	14.47
43-12	Aug. 14, 1994	256.23	−30.8	19.35
43-11	July 11, 1994	261.23	−30.8	21.97
43-10	Dec. 18, 1993	214.82	−37.1	26.66
43-9	Aug. 31, 1993	242.38	−32.3	29.62
43-8	June 24, 1993	260.54	−32.0	31.74
43-7	March 21, 1993	222.15	−44.6	37.11
43-6	Dec. 18, 1992	220.17	−44.7	40.10
43-5	July 23, 1992	257.32	−34.4	46.96
43-4	April 7, 1992	215.47	−41.7	53.40
43-3	Nov. 28, 1991	216.02	−40.4	57.32
43-2	Sept. 3, 1991	230.02	−35.2	61.18
43-1	July 13, 1991	256.22	−31.8	64.12

best available approaches capable of estimating subseasonal accumulation (see *Bromwich et al.* [this issue] for improvements to the atmospheric modeling technique).

The annual accumulation values derived from the snow pit data show excellent agreement with the accumulation map for Greenland compiled by *Bales et al.* [2001]. The mean annual accumulation at the four NGT sites is ~17.6 cm/yr (see Figure 7). This is considerably more than the 10.6 cm/yr mean annual accumulation calculated for the four sites from the atmospheric modeling. In addition, the atmospheric modeling suggests that there is a strong gradient in the accumulation across this area (see Figure 7), whereas the snow pit values and regional accumulation maps do not. If the pit values are taken as accurate for the 1991 to 1995 time period, then the modeling achieves no better than 88% of the observed accumulation. The NGT snow pit accumulation values are also closely equivalent to the rates (<20 cm/yr) documented across this area during the 1950s by *Benson* [1962]. One possibility is that the model grid cells actually represent higher and drier locations even though they geographically cover the snow pit sites; an-

Table 2. (continued)

Match Point ID	Match Point Date	SSM/I Calculated Temperature, K	$\delta^{18}O$, ‰	Water Equivalent Depth, cm
		Pit NGT45		
Surface	July 6, 1995	260.47	−27.4	0
45-17	April 9, 1995	235.91	−41.0	4.56
45-16	Jan. 31, 1995	221.61	−43.3	6.59
45-15	Nov. 8, 1994	240.21	−35.1	11.16
45-14	Nov. 2, 1994	229.52	−36.9	13.59
45-13	Oct. 3, 1994	248.94	−33.3	16.76
45-12	July 6, 1994	264.26	−30.6	20.79
45-11	Jan. 28, 1994	220.73	−43.7	28.27
45-10	Oct. 2, 1993	239.35	−36.7	32.40
45-9	June 24, 1993	264.70	−28.9	37.70
45-8	March 5, 1993	224.85	−44.3	42.54
45-7	Jan. 20, 1993	222.78	−44.8	44.44
45-6	Oct. 30, 1992	243.96	−35.3	47.68
45-5	Sept. 16, 1992	244.92	−34.2	50.06
45-4	July 23, 1992	261.47	−31.9	53.40
45-3	April 8, 1992	220.22	−41.1	57.32
45-2	Feb. 7, 1992	215.82	−41.3	59.44
45-1	Oct. 16, 1991	225.26	−38.1	63.12

[a]Match points were determined as illustrated in Figures 4a–4d and described by *Shuman et al.* [1995a, 1998]. SSM/I calculated temperatures were calculated as described by *Shuman et al.* [1995b, 1998]. Water-equivalent depths were derived from each snow pit profile and from NGT42 density data.

other possibility is that the modeling results are not sensitive to a real aspect of the atmospheric system.

As a final aspect of this study, the relative timing of accumulation across this 220-km-long region was assessed. To do this, the mean monthly accumulation rate values for both data sets for all four sites were combined and plotted relative to the monthly interval midpoint date over an arbitrary year (see Figure 8). As first shown by *Shuman et al.* [1995a, Figure 6], these data illustrate in a relative sense the overall timing of accumulation for a generalized "year" at the site. This analysis is intended to partially compensate for the spatial resolution differences between the snow pit and model data and should be considered as just an illustration. Overall, this analysis is generally consistent with previous results showing a tendency for accumulation to peak during the summer and the fall in the interior of Greenland [see *Bromwich et al.*, 1998, Figure 11]. It is important to recognize that these generalized monthly average results show a "smoothed" version of temporally variable and generally short-term meteorological phenomena (note the variability in Figure 6) and they do not represent a true accumulation time series. This visualization approach is considered useful for interpreting the seasonality of accumulation neces-

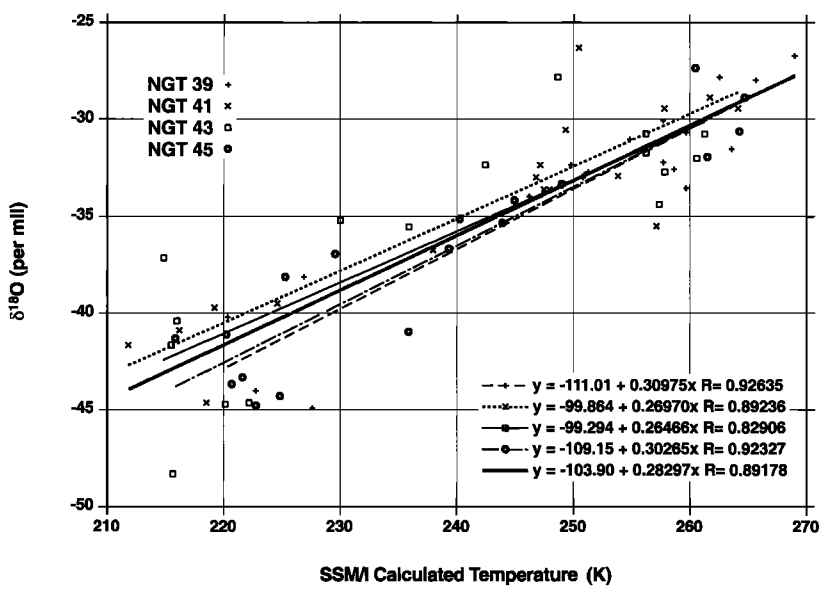

Figure 5. Scatterplot of the pairs of calculated air temperature (T_C) and $\delta^{18}O$ values for the match points from each NGT pit profile (see Table 2). The regression line defines the slope of the T versus δ relationship, ~0.28, for this data set. The regression line slope values presented here are significantly different from the slope value (0.46; 0.39) published by *Shuman et al.* [1995a, 1998].

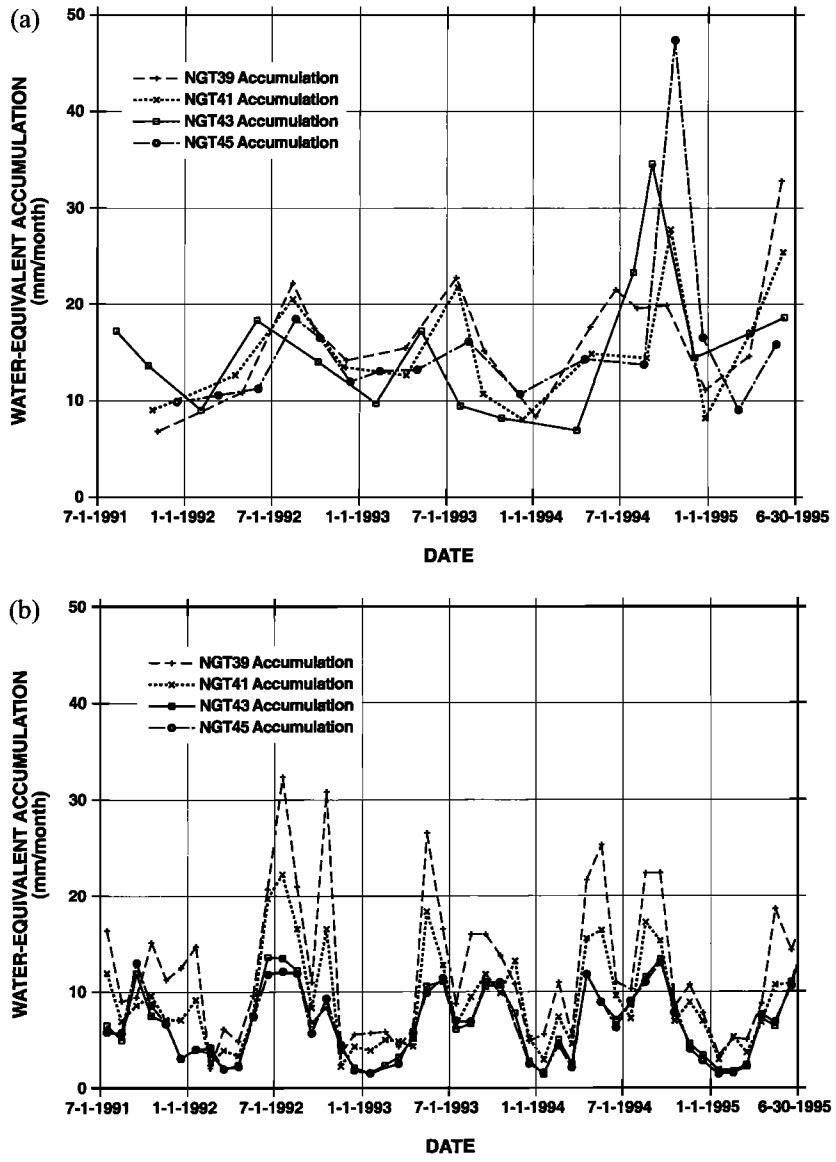

Figure 6. (a) The accumulation time series (mm/month) estimated by the match point technique for the July 1991 to June 1995 time period for each snow pit location. This technique indicates a strong seasonal cycle in accumulation. Note the reduced temporal resolution compared to the model results and the larger peaks in the most recent summer season. (b) The accumulation time series (mm/month) estimated by the atmospheric model for each month of the July 1991 to June 1995 time period for each snow pit location. The trends show that this technique predicts a strong seasonal cycle in accumulation that diminishes from the northern site (NGT39) to the southern site (NGT45). Note the variable peak heights and the double peak that occurs approximately each summer season.

sary for inverting an ice core record [*Steig et al.*, 1994]. The percentage values in Figure 8 indicate the degree of agreement between the two techniques for each month of the arbitrary year. This again assumes that the snow pit observations represent reality.

5. Discussion

The research presented here is consistent with previous efforts [*Shuman et al.*, 1995a, 1998]. It confirms that $\delta^{18}O$ profiles and T_B trends have temporally equivalent primary and secondary features that correspond over a number of years in this area. This result confirms that these latter two records preserve the known annual and subannual variations in temperature for this site. As a result, it appears that in this region, $\delta^{18}O$ is a reliable temperature indicator and that it is preserved in a series of accumulation events that occur frequently throughout the year. This enables, at least over recent multiyear periods, the use of $\delta^{18}O$ as an indicator of paleotemperature for the NGRIP region. Further work will be necessary to know if this multiyear calibration applies to the deeper portions of the NGRIP ice core.

More importantly to PARCA, water-equivalent accumulation data can be derived from the match point data. This details the intra-annual and annual accumulation history for

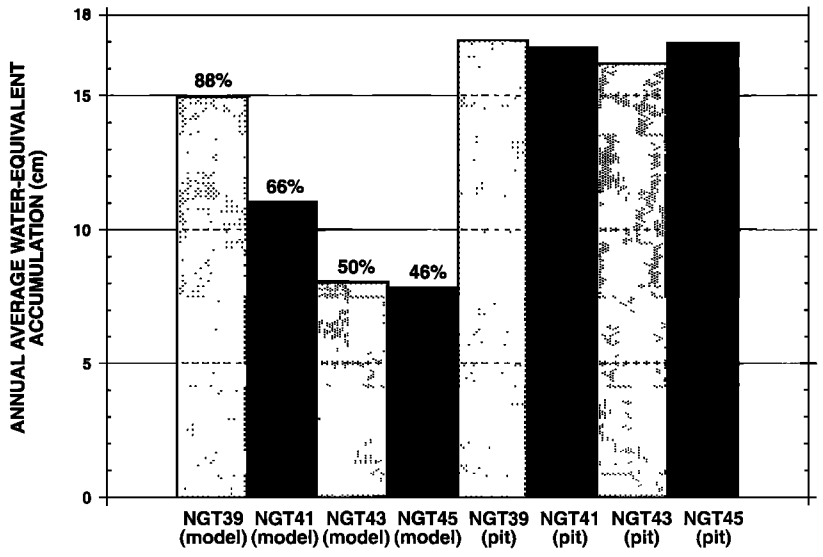

Figure 7. Comparison of the overall magnitudes of the two accumulation measurement techniques for the four NGT sites. The snow pit values are similar in magnitude to published values for this area [*Bales et al.*, 2001]; however, the modeling results are significantly lower.

this region from mid-1991 to mid-1995. The in situ data are consistent with atmospheric modeling results in terms of subseasonal timing but confirm that the magnitude of the modeled precipitation is too low. These snow pit results are comparable to regional analyses of annual accumulation over the past half century as well as to model studies [*Benson*, 1962; *Ohmura and Reeh*, 1991; *Ohmura et al.*, 1996, 1999; *Bales et al.*, 2001].

It should be noted that the match point technique depends on a number of assumptions. First, this approach assumes that all the significant maxima and minima identified in the isotope record are associated temporally with meteorological phenomena that are represented in the brightness temperature record. This assumption is unlikely to be absolutely true and necessarily controls, to some extent, the selection of match points. Specifically, not all "events" in the brightness temperature record have an associated isotope feature, and snow from an event must "accumulate" to provide a match point. This is especially true during periods of low or distinctly intermittent accumulation such as are likely during the winter months. However, it is highly probable that the significant peaks and valleys observed in the AWS and T_B records have accumulation associated with them, possibly within a few days [*Steffensen*, 1985]. Second, even using high-resolution sampling with 3-cm increments, it is likely that there is some diffusion of isotope values through time and therefore the $\delta^{18}O$ record presented here imperfectly represents the actual signal from

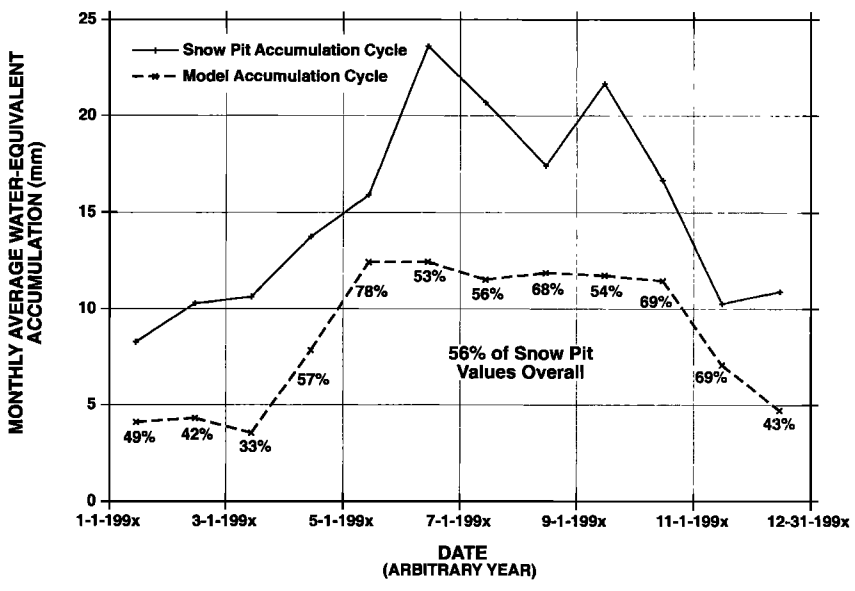

Figure 8. Illustration of the average accumulation cycle for an arbitrary year from the two accumulation measurement techniques for the four NGT sites. Averaging each site's multiyear record of accumulation significantly reduces variability. The modeled values are again lower, but both techniques suggest that accumulation occurs primarily in two pulses during the summer and fall across this region.

the original accumulating snow [*Grootes and Stuiver*, 1997]. Depositional processes act to "homogenize" the near-surface snow through the microscale redistribution of snow grains and water vapor. The ability of the sampling "increment" to capture a specific event that can be matched also plays a role. Note the increased spacing of match points as depth increases in Figure 4 as well as the time period defined by the match points' increases in length. Third, the available density profile was not from each specific snow pit location and is likely to have some error associated with its use. This means the water-equivalent accumulation data are likely to be less precise than is desirable. This may contribute somewhat to the variability in this portion of the analysis (see Figure 6a).

As a result of these problems it is likely that the results determined by the match point technique are not absolutely correct in terms of timing or mass input and therefore the accumulation data should be considered to be estimates with a degree of uncertainty associated with them. Expressed as a percentage, individual values may be in error by 10–20%. Although each concern may be true for any single point in the analysis, it is unlikely that these problems cause a systematic bias to the data, and therefore the overall analysis and its results are still valid. Also, it should be noted that the results presented here are consistent with other annual accumulation estimates, and this suggests that the match point method is a reliable means of investigating the snowpack in central Greenland.

As noted above, the T versus δ regression line slopes from the previous studies [*Shuman et al.*, 1995a, 1998] were higher than the slopes found in this study. One possible explanation of this result is that the slope is generally related to the accumulation across the central Greenland area. Although not published by *Shuman et al.* [1995a, 1998], the multiyear averages for the pits studied were 23.0 and 19.7 cm/yr, compared to 17.6 cm/yr in this study. The regression slope for all points declined from 0.46–0.39 in the first two studies to 0.28 in this study. In other words, lower accumulation may be associated with a lower T versus δ regression slope. The relative consistency of the slope values with relative accumulation within the NGT sites suggests that this result is real (see Figures 5 and 7). However, this may simply be due to greater diffusion occurring as accumulation decreases (snow remains near the snow-air interface longer as it takes more time for a layer to reach a given depth). Another possibility is that there are differences in the source, transport, or fractionation of water vapor that give rise to the observed changes in slope between the GISP 2 or Summit site and the AWI sites near NGRIP. The possibility that the T versus δ regression is sensitive to accumulation and different from the modern spatial gradient (0.67) and recent paleoslope (0.5) values causes concern over how to derive the isotope-temperature relationship for the NGRIP ice core (see further discussion of this problem by *Cuffey and Clow* [1997] and *Jouzel et al.* [1997]).

6. Conclusions

Using independent analysis techniques, accumulation histories for specific ice sheet locations for common time periods have been investigated. Despite significant differences in magnitude (model averages ~56% of observed) and to a lesser extent, timing, these results support the conclusion that accumulation in this area occurs at many times throughout the year and occurs primarily in two pulses during the summer and fall. The seasonal variation in accumulation generally defined here may improve inversion of the NGRIP ice core's paleoclimate record. Application of this approach at other polar ice sheet sites may allow the distribution and timing of accumulation to be estimated with confidence as well as allowing the assessment of the general reliability of isotope thermometry over multiyear periods. The Chen-Bromwich modeling technique, and further variants, may also benefit from these additional validation efforts, allowing confident use of modeling results in areas that cannot be assessed by field techniques.

Acknowledgments. We thank the Alfred Wegener Institut North Greenland Traverse team for their collaboration. We also thank Koni Steffen and Jason Box of the Greenland Climate Network for the NGRIP AWS temperature record. This research was supported by the NASA Program for Arctic Regional Climate Assessment, NASA code YS, and the Earth Observing System Interdisciplinary Science grant 622-1418 to C. A. S. and NASA grant NAG5-6001 to D. H. B. This project was begun while the first author was with NASA Goddard Space Flight Center's Ocean and Ice Branch as a National Research Council Resident Research Associate and Universities Space Research Association Visiting Research Fellow.

References

Abdalati, W., and K. Steffen, Snow melt on the Greenland ice sheet as derived from passive microwave data, *J. Clim.*, *10*, 165–175, 1997.

Abdalati, W., and K. Steffen, Accumulation and hoar effects on microwave emission in the Greenland ice-sheet dry-snow zones, *J. Glaciol.*, *44*(148), 523–531, 1998.

Abdalati, W., R. Bales, and R. Thomas, Program for Arctic Regional Climate Assessment: An improved understanding of the Greenland ice sheet, *Arct. Res. U.S.*, *12*, 38–54, 1998.

Alley, R. B., E. S. Saltzman, K. M. Cuffey, and J. J. Fitzpatrick, Summertime formation of depth hoar in central Greenland, *Geophys. Res. Lett.*, *17*(12), 2393–2396, 1990.

Armstrong, R. L., A. T. C. Chang, A. Rango, and E. Josberger, Snow depths and grain-size relationships with relevance for passive microwave studies, *Ann. Glaciol.*, *17*, 171–176, 1993.

Bales, R. C., J. R. McConnell, E. Mosley-Thompson, and G. Lamorey, Accumulation map for the Greenland ice sheet: 1971–1990, *Geophys. Res. Lett.*, *15*(1), 207–225, 2001.

Benson, C. S., Stratigraphic studies in the snow and firn of the Greenland ice sheet, *SIPRE Res. Rep. 70*, U.S. Army Corps of Eng., Hyattsville, Md., 1962.

Bromwich, D. H., R. I. Cullather, Q. Chen, and B. M. Csathó, Evaluation of recent precipitation studies for Greenland ice sheet, *J. Geophys. Res.*, *103*(D20), 26,007–26,024, 1998.

Bromwich, D. H., Q. Chen, L.-S. Bai, E. N. Cassano, and Y. Li, Modeled precipitation variability over the Greenland ice sheet, *J. Geophys. Res.*, this issue.

Bromwich, D. H., F. M. Robasky, R. A. Keen, and J. F. Bolzan, Modeled variations in precipitation over the Greenland ice sheet, *J. Clim.*, *6*, 1253–1268, 1993.

Chang, A. T. C., P. Gloersen, T. T. Wilheit, and H. J. Zwally, Microwave emission from snow and glacier ice, *J. Glaciol.*, *16*(74), 23–39, 1976.

Charles, C. D., D. Rind, J. Jouzel, R. D. Koster, and R. G. Fairbanks, Glacial-interglacial changes in moisture sources for Greenland: Influences on the ice core record of climate, *Science*, *263*, 508–511, 1994.

Chen, Q., D. H. Bromwich, and L. Bai, Precipitation over Greenland retrieved by a dynamic method and its relation to cyclonic activity, *J. Clim.*, *10*, 839–870, 1997.

Cuffey, K. M., and G. D. Clow, Temperature, accumulation, and ice sheet elevation in central Greenland through the last deglacial transition, *J. Geophys. Res.*, *102*(C12), 26,383–26,396, 1997.

Cuffey, K. M., R. B. Alley, P. M. Grootes, and S. Anandakrishnan, Toward using borehole temperatures to calibrate an isotopic paleothermometer in central Greenland, *Global Planet. Change*, *98*, 265–268, 1992.

Cuffey, K. M., R. B. Alley, P. M. Grootes, J. M. Bolzan, and S. Anandakrishnan, Calibration of the $\delta^{18}O$ isotopic paleothermometer for central Greenland, using borehole temperatures, *J. Glaciol.*, *40*(135), 341–349, 1994.

Dansgaard, W., Stable isotopes in precipitation, *Tellus*, *14*, 436–468, 1964.

Dansgaard, W., S. J. Johnsen, H. B. Clausen, and N. Gundestrup, Stable isotope glaciology, *Medd. Groenl.*, *197*(2), 53 pp., 1973.

Dansgaard, W., H. B. Clausen, N. Gundestrup, S. J. Johnsen, and C. Rygner, Dating and climatic interpretation of two deep Greenland ice cores, in *Greenland Ice Core: Geophysics, Geochemistry, and the Environment*, *Geophys. Monogr. Ser.*, vol. 33, edited by C. C. Langway Jr., H. Oeschger, and W. Dansgaard, pp. 71–76, AGU, Washington, D. C., 1985.

Epstein, S., and R. P. Sharp, Six-year record of oxygen and hydrogen isotope variations in South Pole firn, *J. Geophys. Res.*, *70*(8), 1809–1814, 1965.

Fischer, H., M. Werner, D. Wagenbach, M. Schwager, T. Thorsteinsson, F. Wilhelms, and J. Kipfstuhl, Little ice age clearly recorded in northern Greenland ice cores, *Geophys. Res. Lett.*, *25*(10), 1749–1752, 1998a.

Fischer, H., D. Wagenbach, and J. Kipfstuhl, Sulfate and nitrate firn concentrations on the Greenland ice sheet, 1, Large-scale geographical deposition changes, *J. Geophys. Res.*, *103*(D17), 21,927–21,934, 1998b.

Fischer, H., D. Wagenbach, and J. Kipfstuhl, Sulfate and nitrate firn concentrations on the Greenland ice sheet, 2, Temporal anthropogenic deposition changes, *J. Geophys. Res.*, *103*(D17), 21,935–21,942, 1998c.

Fisher, D. A., R. M. Koerner, W. S. B. Paterson, W. Dansgaard, N. Gundestrup, and N. Reeh, Effect of wind scour on climatic records from ice-core oxygen-isotope profiles, *Nature*, *301*, 205–209, 1983.

Friedman, I., C. Benson, and J. Gleason, Isotopic changes during snow metamorphism, in *Stable Isotope Geochemistry*, edited by H. P. Taylor Jr., J. R. O'Neil, and I. R. Kaplan, *Spec. Publ. Geochem. Soc.*, *3*, 211–221, 1991.

Gardner, T. W., D. W. Jorgensen, C. A. Shuman, and C. Lemieux, Geomorphic and tectonic process rates: Effects of measured time interval, *Geology*, *15*, 259–261, 1987.

Grootes, P. M., and M. Stuiver, $^{18}O/^{16}O$ variability in Greenland snow and ice with 10^{-3}- to 10^{5}-year time resolution, *J. Geophys. Res.*, *102*(C12), 26,455–26,470, 1997.

Hall, D. K., and J. Martinec, *Remote Sensing of Snow and Ice*, 189 pp., Chapman and Hall, New York, 1985.

Hammer, C. U., H. B. Clausen, W. Dansgaard, N. Gundestrup, S. J. Johnsen, and N. Reeh, Dating of Greenland ice cores by flow models, isotopes, volcanic debris, and continental dust, *J. Glaciol.*, *20*(82), 3–26, 1978.

Hollinger, J. P., J. L. Pierce, and G. A. Poe, SSM/I instrument evaluation, *IEEE Trans. Geosci. Remote Sens.*, *28*(5), 781–790, 1990.

Johnsen, S. J., Stable isotope homogenization of polar firn and ice, in *Isotopes and Impurities in Snow and Ice*, Proceedings of the Grenoble Symposium, August/September 1975, *IAHS AISH Publ.*, *118*, 210–219, 1977.

Johnsen, S. J., W. Dansgaard, and J. W. C. White, The origin of Arctic precipitation under present and glacial conditions, *Tellus, Ser. B*, *41*, 452–468, 1989.

Johnsen, S. J., et al., Stable isotope record from deep cores: The climate signal and the role of diffusion, in *Ice Physics and the Natural Environment*, *NATO ASI Ser.*, Ser. 1, vol. 56, edited by J. S. Wettlaufer, J. G. Dash, and N. Untersteiner, pp. 89–107, Springer-Verlag, New York, 1999.

Johnsen, S. J., et al., Diffusion of stable isotopes in polar firn and ice: The isotopic effect in firn diffusion, in *Physics of Ice Core Records*, edited by T. Honodoh, pp. 121–140, Hokkaido Univ. Press, Sapporo, Japan, 2000.

Jouzel, J., et al., On the validity of the temperature reconstruction from water isotopes in ice cores, *J. Geophys. Res.*, *102*(C12), 26,471–26,488, 1997.

Kato, K., Factors controlling oxygen isotopic composition of fallen snow in Antarctica, *Nature*, *272*, 46–48, 1978.

Loewe, F., The Greenland ice cap as seen by a meteorologist, *Q. J. R. Meteorol. Soc.*, *62*, 359–377, 1936.

Maslanik, J. A., J. R. Key, and R. G. Barry, Merging AVHRR and SMMR data for remote sensing of ice and cloud in polar regions, *Int. J. Remote Sens.*, *10*(10), 1691–1696, 1989.

McConnell, J. R., E. Mosley-Thompson, D. H. Bromwich, R. C. Bales, and J. D. Kyne, Interannual variations of snow accumulation on the Greenland ice sheet (1985–1996): New observations versus model predictions, *J. Geophys. Res.*, *105*(D3), 4039–4046, 2000.

National Snow and Ice Data Center (NSIDC), DMSP SSM/I brightness temperature and sea ice concentration grids for the polar regions on CD-ROM, User's Guide, *Spec. Rep. 1*, Coop. Inst. for Res. in Environ. Sci., Univ. of Colo., Boulder, 1992.

Newell, R. E., and Y. Zhu, Tropospheric rivers: A one-year record and a possible application to ice core data, *Geophys. Res. Lett.*, *21*(2), 113–116, 1994.

Ohmura, A., and N. Reeh, New precipitation and accumulation maps for Greenland, *J. Glaciol.*, *37*(125), 140–148, 1991.

Ohmura, A., et al., A possible change in mass balance of Greenland and Antarctic ice sheets in the coming century, *J. Clim.*, *9*, 2124–2135, 1996.

Ohmura, A., et al., Precipitation, accumulation, and mass balance of the Greenland ice sheet, *Z. Gletscherk. Glazialgeol.*, *35*(1), 1–20, 1999.

Petit, J. R., J. W. C. White, N. W. Young, J. Jouzel, and Y. S. Korotkevich, Deuterium excess in recent Antarctica snow, *J. Geophys. Res.*, *96*(D3), 5113–5122, 1991.

Rott, H., K. Sturm, and H. Miller, Active and passive microwave signatures of Antarctic firn by means of field measurements and satellite data, *Ann. Glaciol.*, *17*, 337–343, 1993.

Schwager, M., Eisbohrkernuntersuchungen zur räumlichen und zeitlichen Variabilitat von Temperatur und Niederschlagsrate im Spätolozän in Nordgrönland (Ice core analysis on the spatial and temporal variability of temperature and precipitation during the late Holocene in North Greenland), Ph.D. thesis, Alfred Wegener Inst., Univ. of Bremen, Bremen, Germany, 1999.

Shuman, C. A., and R. B. Alley, Spatial and temporal characterization of hoar formation in central Greenland using SSM/I brightness temperatures, *Geophys. Res. Lett.*, *20*(23), 2643–2646, 1993.

Shuman, C. A., R. B. Alley, S. Anandakrishnan, J. W. C. White, P. M. Grootes, and C. R. Stearns, Temperature and accumulation at the Greenland summit: Comparison of high-resolution isotope profiles and satellite passive microwave brightness temperature trends, *J. Geophys. Res.*, *100*(D5), 9165–9177, 1995a.

Shuman, C. A., R. B. Alley, S. Anandakrishnan, and C. R. Stearns, An empirical technique for estimating near-surface air temperatures in central Greenland from SSM/I brightness temperatures, *Remote Sens. Environ.*, *51*, 245–252, 1995b.

Shuman, C. A., R. B. Alley, M. A. Fahnestock, R. A. Bindschadler, J. W. C. White, J. R. McConnell, and J. Winterle, Temperature history and accumulation timing for the snow pack at GISP2, central Greenland, *J. Glaciol.*, *44*(146), 21–30, 1998.

Shuman, C. A., M. A. Fahnestock, R. A. Bindschadler, R. B. Alley, and C. R. Stearns, A dozen years of temperature observations at the Summit: Central Greenland automatic weather stations 1987–1999, *J. Appl. Meteorol.*, *40*(4), 741–752, 2001.

Shuman, C. A., R. B. Alley, M. A. Fahnestock, P. J. Fawcett, R. A. Bindschadler, S. Anandakrishnan, and C. R. Stearns, Detection and monitoring of annual indicators and temperature trends at GISP2 using passive microwave remote sensing data, *J. Geophys. Res.*, *102*(C12), 26,877–26,886, 1997.

Sommerfeld, R. A., C. Judy, and I. Friedman, Isotopic changes during the formation of depth hoar in experimental snowpacks, in *Stable Isotope Geochemistry*, edited by H. P. Taylor Jr., J. R. O'Neil, and I. R. Kaplan, *Spec. Publ. Geochem. Soc.*, *3*, 205–209, 1991.

Steffen, K., J. E. Box, and W. Abdalati, Greenland Climate Network: GC-Net, in *Glaciers, Ice Sheets, and Volcanoes: A Tribute to Mark F. Meier*, edited by S. C. Colbeck, *CRREL Spec. Rep.*, *96-27*, 98–103, 1996.

Steffensen, J. P., Microparticles in snow from the south Greenland ice sheet, *Tellus, Ser. B*, *37*, 286–295, 1985.

Steig, E. J., P. M. Grootes, and M. Stuiver, Seasonal precipitation timing and ice core records, *Science*, *266*, 1885–1886, 1994.

Whillans, I. M., and P. M. Grootes, Isotopic diffusion in cold snow and firn, *J. Geophys. Res.*, *90*(D2), 3910–3918, 1985.

White, J. W. C., L. K. Barlow, D. Fisher, P. Grootes, J. Jouzel, S. J. Johnsen, M. Stuiver, and H. Clausen, The climate signal in the stable isotopes of snow from Summit, Greenland: Results of comparisons

with modern climate observations, *J. Geophys. Res.*, *102*(C12), 26,425–26,439, 1997.

Zwally, H. J., and S. Fiegles, Extent and duration of Antarctic surface melting, *J. Glaciol.*, *40*(136), 463–476, 1994.

D. H. Bromwich, Byrd Polar Research Center, 1090 Carmack Road, Ohio State University, Columbus, OH 43210-1308, USA. (bromwich@polarmet1.mps.ohio-state.edu)

J. Kipfstuhl and M. Schwager, Alfred-Wegener-Institut für-Polar und Meeresforschung, Columbusstrasse, D-27568, Bremerhaven, Germany. (kipfstuhl@awi-bremerhaven.de)

C. A. Shuman, NASA Goddard Space Flight Center, Building 33, Room A210, Code 971, Oceans and Ice Branch, Greenbelt, MD 20771, USA. (christopher.shuman@gsfc.nasa.gov)

(Received July 31, 2000; revised February 28, 2001; accepted March 21, 2001.)